Suspended core photonic microcells for sensing and device applications

Chao Wang, Wei Jin,* Jun Ma, Ying Wang, Hoi Lut Ho, and Xin Shi

Department of Electrical Engineering, The Hong Kong Polytechnic University, Hung Hom, Kowloon, Hong Kong
Corresponding author: eewjin@polyu.edu.hk

In-line fiber-optic microcells are fabricated by postprocessing NKT LMA10 photonic crystal fibers. The cells are suspended core (SC) elements created by locally inflating some of the air holes while the core is being tapered. Based on a SC microcell with six air holes, a cantilever beam accelerometer is demonstrated. The microcells could also be used as gain and absorption cells for amplifier and spectroscopy applications.   © 2013 Optical Society of America

OCIS codes: (060.2340) Fiber optics components; (060.2370) Fiber optics sensors; (060.4005) Microstructured fibers; (060.5295) Photonic crystal fibers.
http://dx.doi.org/10.1364/OL.38.001881

Optical fibers with a micrometer/nanometer size core suspended by extremely thin webs connected to a thicker outer cladding provide an ideal platform for light-matter interaction through an evanescent field. These suspended core fibers (SCFs) have been studied for absorption-based gas and liquid detection, fluorescent material excitation, and sensing [1,2]. Compared with bare micrometer/nanometer wires, an SCF is more robust since its core is isolated from the external environment by the outer cladding that also serves as a container for gas/liquid samples. The shape and size of the SCF's core can be designed to achieve high birefringence and/or nonlinear properties [3,4].

However, because of the special geometry and much smaller core size, the mode field of an SCF is typically very different from a normal-sized fiber. A joint or splice between the two types of fibers is typically associated with large optical loss. In this Letter, we report a technique for making low-loss in-line suspended core (SC) microcells by postprocessing a commercial photonic crystal fiber (PCF). The microcells have the properties of an SCF but are automatically connected to normal-size PCF pigtails from which they are made, making it easier to integrate them into conventional fiber optic systems.

There have been reports on postprocessing stock PCFs to modify its local waveguide properties and create photonic devices. These include the fabrication of in-line modal interferometers [5], the creation of local high birefringence [6], anamorphic core-shape transitions [7], and nonlinear applications [4]. However, in these previous works, the fiber cores are still embedded within modified periodic cladding microstructures. Different from previous works, we report here a much larger scale modification of the cladding structure to locally create a microcell with a "SC".

The process of fabricating the microcells may be explained with the aid of Fig. 1. The first step is to seal or open selected air columns of a PCF. Several methods for this purpose have been reported [6–10]. Here, we adopted the femtosecond drilling method [6,8], which selectively opens a minority of air holes. The PCF used here is the NKT LMA-10 fiber with a core diameter of 10.1 ± 0.5 μm, the cladding hole diameter and pitch are ~3.3 μm and 7.2 μm, respectively. The photo on

the left in Fig. 1(a) shows the end view of the PCF with the innermost 6 holes opened while the other holes are tightly sealed by a short section of single mode fiber (SMF) spliced to the PCF. The other end of the PCF is spliced to a longer SMF. The PCF end with opened holes is then sealed into a gas chamber [Fig. 1(b)] and the opened air holes are pressurized, while the other holes remain at atmospheric pressure. The PCF is then heated locally and the holes with higher gas pressure will expand gradually, while those with lower pressure holes
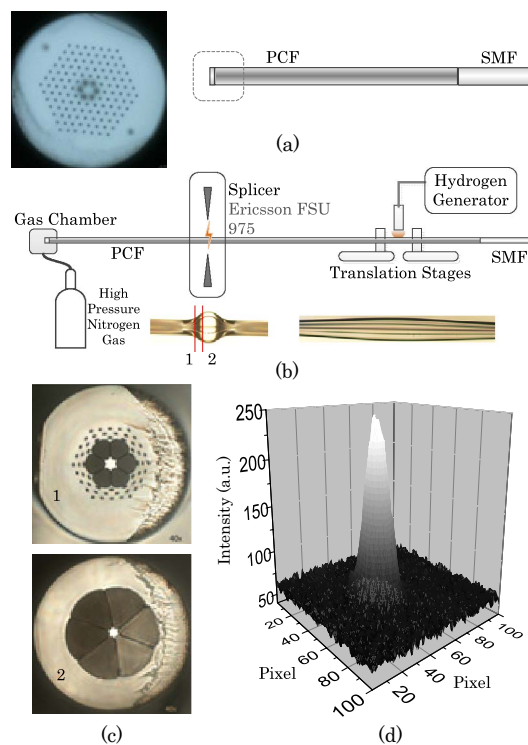

Fig. 1.   (a) Selective opening of air-holes from PCF end. (b) Selective inflation of air holes by pressurizing the opened hole while the PCF is being heated and drawn. Photo on the left shows the side view of a microcell created by an electric arc discharge, while the one on the right is created by flame brushing. (c) Cross section of the microcell created by an arc discharge at two different locations, 1 and 2. (d) Measured near-field image at location 2 at 1550 nm.

will collapse. To keep a hole in a silica PCF from collapsing due to surface tension, the pressure should be larger than 6/d (micrometer), where d is the diameter of hole [4]; for the LMA-10 PCF, it's ~2 bar.

Either an electric arc discharge or an oxy-hydrogen flame may be used as the heating source, both of which are suitable for creating shorter (<1 mm) and longer (1–7 cm, realized in experiment) lengths of SC elements, respectively. The photo on the lower left panel in Fig. 1(b) shows the side view of a ~600 μm long microcell created by arc discharge from a fusion splicer with a gas pressure of 3 bar. Gentle drawing is applied during the discharge to ensure a straight SC and gradual reduction of the core diameter (adiabatic taper). The photo on the lower right panel in Fig. 1(b) is a ~10 mm long microcell created by the flame brushing method. Figure 1(c) shows the cross section of the ~600 μm long microcell at two different locations, 1 and 2. The taper transition length of this particular cell is ~100 μm and the radius at the waist is ~3.5 μm. Fig. 1(d) shows the mode intensity image at location 2 at 1550 nm, taken by an infrared CCD camera. The light energy is predominantly in the fundamental mode, and coupling to higher order modes is negligible.

To monitor the optical quality of the microcells, *in situ* monitoring of the light transmission is needed. For this purpose, a two-step process is used: a microcell is first created by following the procedure in Fig. 1. A femtosecond infrared laser is then used to drill holes on the sidewall of the microcell [11]. The purpose of this is to create lateral openings on the inflated holes that will serve as channels to apply gas pressure to selected holes columns while leaving the input/output ends free for connection to a light source and an optical spectrum analyzer (OSA) via SMF pigtails, as shown in Fig. 2(a). Local heating by either arc discharge or flame brushing is then applied to a new location as indicated in Fig. 2(a) and a second microcell is created. The transmission characteristics of the second cell are completely determined, and it would be more convenient to use such a cell in practical applications. Figure 2(b) shows the cross section of two typical microcells made by inflating 4 and 3 air holes, respectively. These cells have a typical loss of less than 0.2 dB and may be used as low-loss photonic cells for absorption/fluorescent spectroscopy, gain cells for fiber amplifiers and lasers, as well as cells for refractive index sensors. Note that the 0.2 dB loss does not include the loss of the two splices between the LMA-10 and the SMFs, which is ~1.5 dB in total and may be further reduced by optimizing splicing procedures [12]. The drilling of holes from the side wall was found to introduce negligible loss to the microcell.
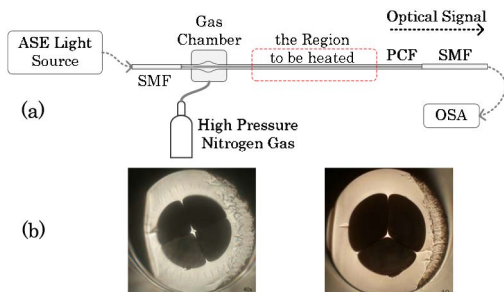
As an example of potential applications of the microcells, we demonstrated a cantilever beam accelerometer as illustrated in Fig. 3. An in-line microcell with an SC is first made by using the flame brushing method; the SC is then cut by a femtosecond laser so that a small gap is introduced between the two sections of the core. The surrounded struts of one section are also removed by scanning the focused femtosecond laser beam across them, resulting in a cantilever beam as shown in Fig. 3. The cantilever deflects with applied acceleration, resulting in misalignment between the two sections of the core and modulates the transmitted light intensity. An important advantage of this design is that the whole cantilever beam is encapsulated in the microcell, making it easier to mount as well as free from contamination from the outside environment.

Because of the adiabatic profile of the tapered SC, only the fundamental mode exists in the tapered region. The optical transmission as a function as lateral offset of the free cantilever end may be estimated by calculating the mode field with COMSOL FEM software, fitting the field to a Gaussian distribution and calculating the coupling coefficient with consideration of the offset, tilt, and longitudinal separation between the two sections of the SC [13]. For the structure shown in Fig. 3(b), the cantilever beam is ~1.35 mm long and the gap between the two sections of the core is ~5 μm. The transmission coefficient is calculated and shown in Fig. 4. In the region marked in red, the optical transmission exhibits a quasilinear response to the free end offset. To make the device work in this region, we purposely introduce an initial offset by using the femtosecond laser to pare the beam's strut remnants from one side. This can be accomplished by monitoring the optical attenuation (2–3 dB) during the
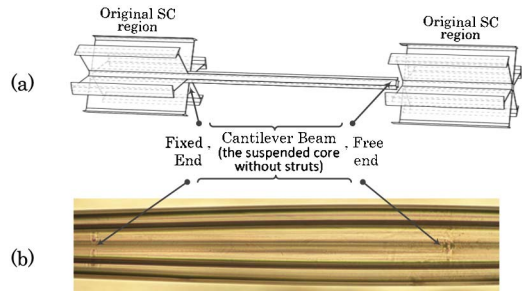

Fig. 3.   (a) Schematic of the SC within the microcell. (b) Photo of a device showing the gap between the two sections of the SC.
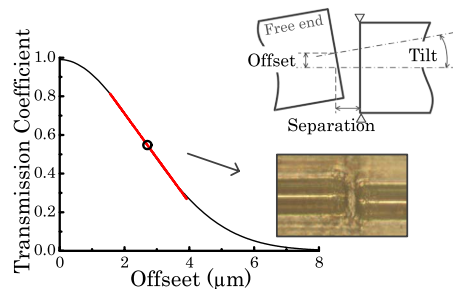

Fig. 4.   Optical power transmission coefficient versus offset at the cantilever beam free end (the effect of tilt and separation are included). Schematic and photo show the offset at the cantilever free end. Core on the right remains suspended by the struts.
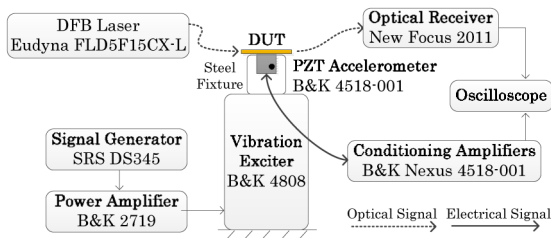

Fig. 2.   (a) Setup for fabricating a microcell with *in situ* monitoring of its transmission. (b) Examples of SC microcells fabricated.

Fig. 5. Setup for testing the in-line accelerometer. DUT is the cantilever beam accelerometer.

process of fine paring. The inset photo in Fig. 4 illustrates the initial offset at the cantilever free end.

Under the assumption of small deflection, the deflection of the beam's free end is a linear function of acceleration with its sensitivity coefficient proportional to the 4th power of beam length [14], indicating the device could be made more sensitive by using a longer beam.

Preliminary tests of the in-line accelerometer were conducted with the setup shown in Fig. 5. Light from a 1530 nm DFB laser is delivered to the microcell (device under test or DUT) and the output is collected by a photo receiver. The DUT is fixed to a vibration exciter by use of a steel fixture, and a commercial piezoelectric accelerometer is attached to the same fixture to provide accurate real-time calibration of the acceleration applied.

Figure 6(a) shows the oscilloscope traces measured with the reference and the cantilever beam accelerometers when a 100 Hz excitation signal is applied. The sensitivity of the reference accelerometer is 31.6 mV/g, and the optical receiver has a conversion coefficient of 0.56V/mW. Figure 6(b) shows the output amplitudes of the fiber-optic accelerometer as functions of acceleration for an applied frequency of 100 Hz and 1 kHz. Good linear relationships were obtained within the test range from 0.01 to 5 g. This is about one third of the range reported in [15]; however, it is not limited by the accelerometer but rather the experimental setup. Theoretical calculation based on the linear region of Fig. 4 indicates that the linear response range could reach 60 and 58.4 g for 100 Hz and 1 kHz, respectively. Figure 6(c) shows the frequency response of the fiber-optic accelerometer. A resonant peak appears at ~6.6 kHz, and the response is flat until ~2.5 kHz with a sensitivity of ~2.6 mV/g. For frequencies closer to the resonant peak, the sensitivity would increase significantly but the linear response range would decrease. The inset in Fig. 6(c) shows the spectrum of the fiber-optic accelerometer output when an acceleration of 10 mg in amplitude and 100 Hz in frequency is applied. The resolution bandwidth is set to 2 Hz. The signal to noise ratio at 100 Hz is ~35.5 dB, from which the minimum detectable acceleration corresponding to SNR = 1 is calculated to be 119 $\mu g/(Hz)^{1/2}$.

In summary, we reported the fabrication of an in-fiber photonic microcell with a SC by postprocessing a commercial PCF. Based on such a microcell, a compact in-line fiber-optic cantilever beam accelerometer is demonstrated. The photonic microcells may be useful components for absorption/florescent-based spectroscopic sensors and refractive index sensors, as well as gain cells for future fiber amplifiers and laser systems.
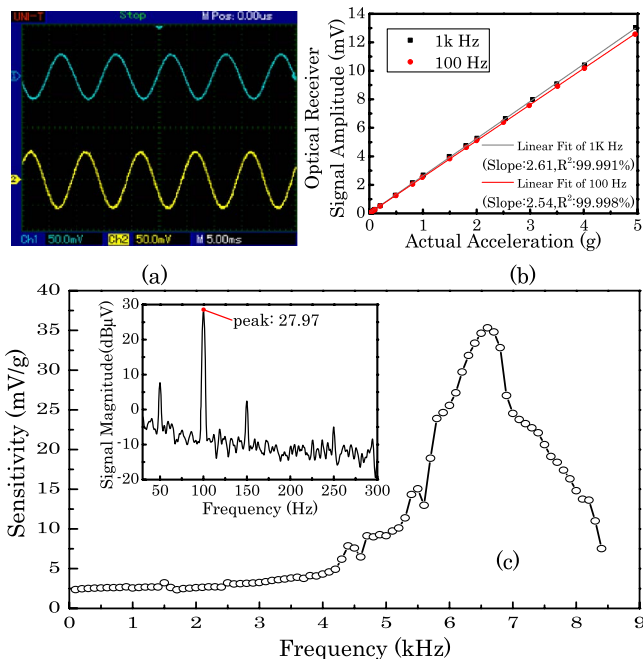

Fig. 6. (a) Oscilloscope traces showing the outputs from the piezoelectric (upper) and the fiber-optic (lower) accelerometers. Output from the optical receiver is amplified 30 times before being connected to the oscilloscope. (b) Magnitude of fiber-optic accelerometer output versus acceleration (obtained from the piezoelectric accelerometer). (c) Frequency response of the fiber-optic accelerometer. Inset graph: output spectrum when an acceleration of 10 mg (amplitude) at 100 Hz is applied.

References
1. O. Frazão, R. M. Silva, M. S. Ferreira, J. L. Santos, and A. B. Lobo Ribeiro, Photonic Sens. **2**, 118 (2012).
2. Y. Zhu, H. Du, and R. Bise, Opt. Express **14**, 3541 (2006).
3. L. Dong, B. K. Thomas, and L. Fu, Opt. Express **16**, 16423 (2008).
4. W. Wadsworth, A. Witkowska, S. Leon-Saval, and T. A. Birks, Opt. Express **13**, 6541 (2005).
5. R. M. Gerosa, D. H. Spadoti, L. D. S. Menezes, and C. J. de Matos, Opt. Express **19**, 3124 (2011).
6. J. Ju, H. F. Xuan, W. Jin, S. Liu, and H. L. Ho, Opt. Lett. **35**, 3886 (2010).
7. A. Witkowska, K. Lai, S. G. Leon-Saval, W. J. Wadsworth, and T. A. Birks, Opt. Lett. **31**, 2672 (2006).
8. Y. Wang, C. R. Liao, and D. N. Wang, Opt. Express **18**, 18056 (2010).
9. M. Vieweg, T. Gissibl, S. Pricking, B. T. Kuhlmey, D. C. Wu, B. J. Eggleton, and H. Giessen, Opt. Express **18**, 25232 (2010).
10. F. Wang, S. W. Yuan, O. Hansen, and O. Bang, Opt. Express **19**, 17585 (2011).
11. Y. L. Hoo, S. Liu, H. L. Ho, and W. Jin, IEEE Photon. Technol. Lett. **22**, 296 (2010).
12. L. Xiao, M. S. Demokan, W. Jin, Y. Wang, and C. L. Zhao, J. Lightwave Technol. **25**, 3563 (2007).
13. D. Marcuse, Bell Syst. Tech. J. **56**, 703 (1977).
14. J. M. Gere and B. J. Goodno, *Mechanics of Materials* (CL-Engineering, 2009).
15. A. Stefani, S. Andresen, W. Yuan, N. Hergoldt-Rasmussen, and O. Bang, IEEE Photon. Technol. Lett. **24**, 763 (2012).